

SCWR Once-Through Calculations for Transmutation and Cross Sections

Francesco Ganda

July 2012



The INL is a U.S. Department of Energy National Laboratory
operated by Battelle Energy Alliance

INL/EXT-12-26622
FCRD-FCO-2012-000184

SCWR Once-Through Calculations for Transmutation and Cross Sections

Francesco Ganda

July 2012

**Idaho National Laboratory
Fuel Cycle Research & Development
Idaho Falls, Idaho 83415**

<http://www.inl.gov>

**Prepared for the
U.S. Department of Energy
Assistant Secretary for Fossil Energy
Under DOE Idaho Operations Office
Contract DE-AC07-05ID14517**

DISCLAIMER

This information was prepared as an account of work sponsored by an agency of the U.S. Government. Neither the U.S. Government nor any agency thereof, nor any of their employees, makes any warranty, expressed or implied, or assumes any legal liability or responsibility for the accuracy, completeness, or usefulness, of any information, apparatus, product, or process disclosed, or represents that its use would not infringe privately owned rights. References herein to any specific commercial product, process, or service by trade name, trade mark, manufacturer, or otherwise, does not necessarily constitute or imply its endorsement, recommendation, or favoring by the U.S. Government or any agency thereof. The views and opinions of authors expressed herein do not necessarily state or reflect those of the U.S. Government or any agency thereof.

SUMMARY

It is the purpose of this report to document the calculation of (1) the isotopic evolution and of (2) the 1-group cross sections as a function of burnup of the reference Super Critical Water Reactor (SCWR), in a format suitable for the Fuel Cycle Option Campaign Transmutation Data Library. The reference SCWR design was chosen to be that described in [McDonald, 2005].

Super Critical Water Reactors (SCWR) are intended to operate with super-critical water (i.e. H₂O at a pressure above 22 MPa and a temperature above 373°C) as a cooling – and possibly also moderating – fluid. The main mission of the SCWR is to generate lower cost electricity, as compared to current standard Light Water Reactors (LWR). Because of the high operating pressure and temperature, SCWR feature a substantially higher thermal conversion efficiency than standard LWR – i.e. about 45% versus 33%, mostly due to an increase in the exit water temperature from ~300°C to ~500°C – potentially resulting in a lower cost of generated electricity. The coolant remains single phase throughout the reactor and the energy conversion system, thus eliminating the need for pressurizers, steam generators, steam separators and dryers, further potentially reducing the reactor construction capital cost. The SCWR concept presented here is based on existing LWR technology and on a large number of existing fossil-fired supercritical boilers.

However, it was concluded in [McDonald, 2005], that: “*Based on the results of this study, it appears that the reference SCWR design is not feasible.*” This conclusion appears based on the strong sensitivity of the design to small deviations in nominal conditions leading to small effects having a potentially large impact on the peak cladding temperature of some fuel rods. “*This was considered a major feasibility issue for the SCWR*” [McDonald, 2005]. However, it was beyond the scope of this report to further investigate this issue and to confirm or rebut these findings, since they appear to be mostly based on thermal-hydraulic considerations, while this report is focused on the reactor physics aspects of the design.

After a description of the reference SCWR design, the Keno V 3-D single assembly model used for this analysis, as well as the calculated results, are presented.

Additionally, the following information, presented in the appendixes, is intended to provide enough guidance that a researcher repeating the same task in the future should be able to obtain a vector of nuclei and cross sections ready for insertion into the transmutation library without any need for further instructions:

- (1) Complete TRITON/KENO-V input used for the analysis;
- (2) Inputs and detailed description of the usage of the OPUS utility, used to postprocess and to extract the nuclei concentrations for the transmutation library;
- (3) Inputs and detailed description of the usage of the XSECLIST utility, used to postprocess and to extract the 1-group cross sections for the transmutation library;
- (4) Details of an ad-hoc utility program developed to sort the nuclei and cross sections for the transmutation library.

CONTENTS

SUMMARY	iii
ACRONYMS.....	vii
1. Description of the concept.....	1
1.1 Neutronic computational model used in [McDonald, 2005].....	4
2. Description of the model	8
3. REFERENCES.....	11
APPENDIX A TRITON/KENO-V input for the RBWR model	12
APPENDIX B OPUS input and nuclide concentrations post-processing.....	21
APPENDIX C XSECLIST input and cross sections post-processing.....	22
APPENDIX D SCALE_XSLIST_READER for the conversion of OPUS and XSECLIST outputs to the standard format of the transmutation library	24

FIGURES

Figure 1-1. Conceptual design of the reference SCWR pressure vessel and internals, from [McDonald, 2005].	2
Figure 1-2. The SCWR fuel assembly with metal water rod boxes, from [McDonald, 2005].	4
Figure 2-2. SCWR spectra at BOL in the fuel at the bottom, center and top of the core.....	9
Figure 2-3. Evolution with burnup of the radially-reflected burnup.....	10

TABLES

Table 1-1. Conceptual reference SCWR reference design power and coolant conditions. From [McDonald, 2005].	3
Table 1-2. Reference reactor core design for the reference SCWR. From [McDonald, 2005].....	3
Table 1-3. Reference fuel assembly design for the reference SCWR. From [McDonald, 2005].....	3
Table 1-4. Reference fuel pin design for the reference SCWR. From [McDonald, 2005].	4
Table 1-5. Major elemental constituents for MA956, Alloy 718, Zircaloy-4, and SiC. From [McDonald, 2005].	6
Table 1-6. Assembly lattice k-infinity for four different clad materials. From [McDonald, 2005]......	6
Table 1-7. Converged beginning-of-life SCWR water densities for the coolant. From [McDonald, 2005].....	7

ACRONYMS

BU	Burnup (in GWD/MTiHM)
EFPD	Evaluated Full Power Days
EFPY	Evaluated Full Power Years
GWD/MTiHM	GigawattDays per Metric Ton of Initial Heavy Metal
HM	Heavy Metal
LWR	Light Water Reactor
MT	Metric Ton
PWR	Pressurized Water Reactor
SCWR	Super Critical Water Reactor
XS	Cross Sections

SCWR ONCE-THROUGH CALCULATIONS FOR TRANSMUTATION AND CROSS SECTIONS

It is the purpose of this report to document the calculation of (1) the isotopic evolution and of (2) the 1-group cross sections as a function of burnup of the reference Super Critical Water Reactor (SCWR). The reference SCWR design was chosen to be that described in [McDonald, 2005].

Section 1 provides a description of the reference SCWR design, its main features and the neutronic computational model used in [McDonald, 2005].

Section 2 describes the Keno V 3-D single assembly model used for the results produced for this work. Appendix A provides the complete TRITON/KENO-V input used for the analysis. Appendix B and C provide a detailed description and the inputs of, respectively, the OPUS and XSECLIST post processing used to extract the transmutation library data. Appendix D describes in detail the procedure for using a utility program developed to sort the nuclei and cross sections for the transmutation library.

The description in the appendixes is intended to provide enough guidance that a researcher repeating the same task in the future should be able to obtain a vector of nuclei and cross sections ready for insertion into the transmutation library without any need for further instructions.

1. Description of the concept

Super Critical Water Reactors (SCWR) are intended to operate with super-critical water (i.e. H₂O at a pressure above 22 MPa and a temperature above 373°C) as a cooling – and possibly also moderating – fluid. The main mission of the SCWR is to generate lower cost electricity, as compared to current standard Light Water Reactors (LWR). Because of the high operating pressure and temperature, SCWR feature a substantially higher thermal conversion efficiency than standard LWR – i.e. about 45% versus 33%, mostly due to an increase in the exit water temperature from ~300°C to ~500°C – potentially resulting in a lower cost of generated electricity. The coolant remains single phase throughout the reactor and the energy conversion system, thus eliminating the need for pressurizers, steam generators, steam separators and dryers, further potentially reducing the reactor construction capital cost. The concept is based on existing LWR technology and on a large number of existing fossil-fired supercritical boilers.

However, it was concluded in [McDonald, 2005], that: “Based on the results of this study, it appears that the reference SCWR design is not feasible.” This conclusion appears based on the strong sensitivity of the design to small deviations in nominal conditions leading to small effects having a potentially large impact on the peak cladding temperature of some fuel rods. “This was considered a major feasibility issue for the SCWR” [McDonald, 2005].

The conceptual SCWR design used as reference for this work is shown in Figure 1-1, while the reference design and coolant conditions are shown in Table 1-1 (from [McDonald, 2005]). It is noted in particular the thermal efficiency level of 44.8%, substantially higher than that of standard LWR.

Key characteristics of the design are:

- 25 MPa system pressure;
- Inlet and outlet temperatures of 280°C and 500°C respectively;
- Water density changes across the core from 760 kg/m³ to 90 kg/m³;
- 90% of the total inlet flow goes to the top plenum, and then flows downwards in special water rods to the bottom plenum, where it mixes with the remaining 10% inlet flow before passing through the active core. This arrangement is designed to provide additional moderation in the upper part of the core.

The vessel is similar in dimensions to that of a standard PWR, but thicker because of the higher pressure. The vessel material is envisioned to be SA-533 or SA-508, Grade 3, Class 1, and clad with stainless steel 308 (from [McDonald, 2005]).

The parameters necessary for the neutronic calculations are shown in Tables 1-2 to 1-4 (from [McDonald, 2005]), and a radial view of the reference fuel assembly is shown in Figure 1-2.

Each assembly will have 1 instrumentation tube in the center, and the control rods are inserted in the water channels. Each assembly has 36 water rods and 300 UO_2 active fuel pin; the average linear heat rate is 19.2 kW/m, resulting in a calculated power density of 34.522 W/gHM using the active fuel geometry and the UO_2 density of 10.4215 g/cm³, corresponding to 95% theoretical density. The heated fuel length is 4.26 m.

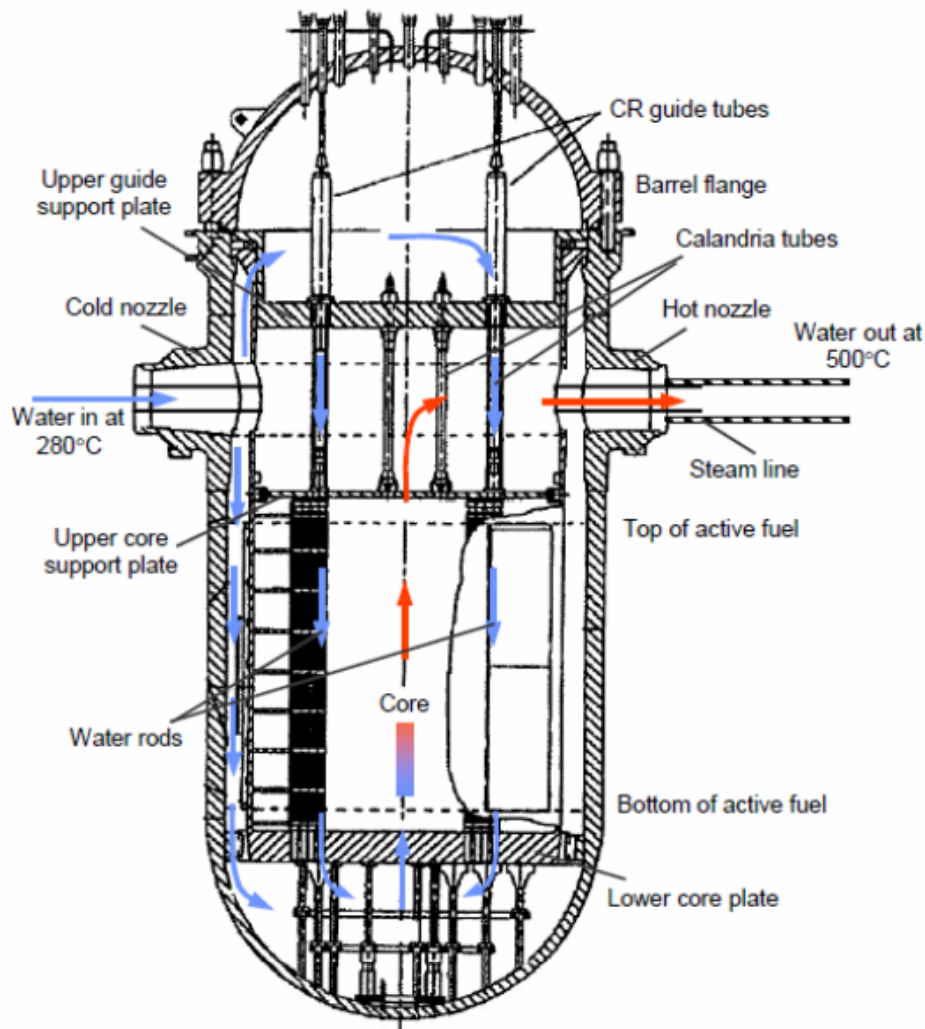


Figure 1-1. Conceptual design of the reference SCWR pressure vessel and internals, from [McDonald, 2005].

Table 1-1. Conceptual reference SCWR reference design power and coolant conditions. From [McDonald, 2005].

Parameter	Value
Thermal power	3575 MWt
Net electric power	1600 MWe
Net thermal efficiency	44.8%
Operating pressure	25 MPa
Reactor inlet temperature	280 °C
Reactor outlet temperature	500 °C
Reactor flow rate	1843 kg/s
Plant lifetime	60 years

Table 1-2. Reference reactor core design for the reference SCWR. From [McDonald, 2005].

Number of fuel assemblies	145
Equivalent diameter	3.93 m
Core barrel inside and outside diameter	4.3/4.5 m
Axial/radial/local/total peaking factor	1.4/1.3/1.1/2.0 (best estimate) 1.4/1.4/1.2/2.35 (safety analysis)
Average power density	69.4 kW/L
Average linear power	19.2 kW/m
Peak linear power at steady-state conditions	39 kW/m
Core pressure drop	0.15 MPa
Water rod flow	1660 kg/s (90% of nominal flow rate)

Table 1-3. Reference fuel assembly design for the reference SCWR. From [McDonald, 2005].

Fuel pin lattice	Square 25×25 array
Number of fuel pins per assembly	300
Pitch-to-diameter ratio	1.09804
Number of water rods per assembly	36
Water rod side	33.6 mm
Water rod wall thickness	0.4 mm
Water rod wall materials	TBD
Number of instrumentation rods per assembly	1
Number of control rod fingers per assembly	12
Control rod material	B ₄ C
Number of spacer grids	14
Assembly wall thickness	3 mm
Assembly wall material	TBD
Assembly side	286 mm
Inter-assembly gap	2 mm
Assembly pitch	288 mm

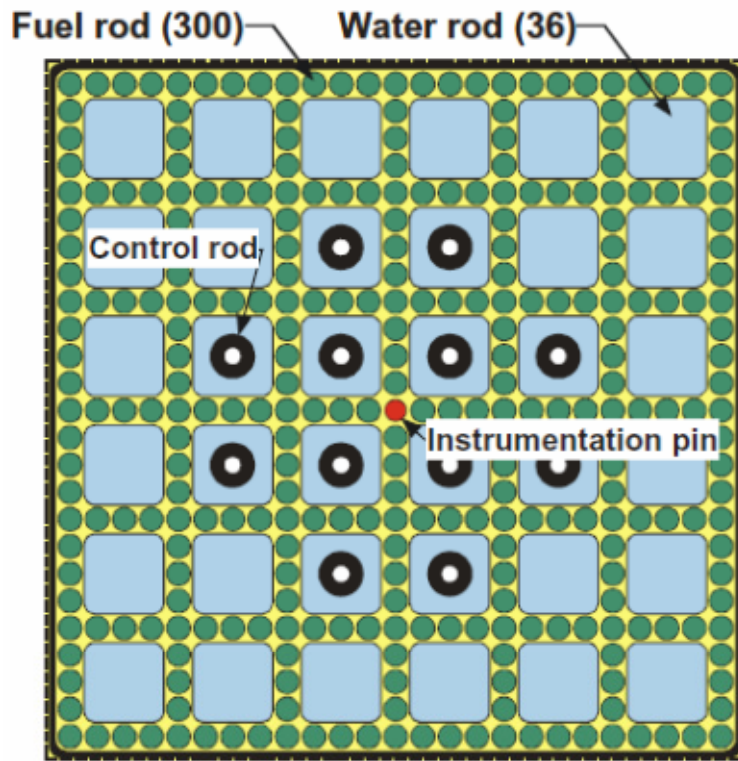


Figure 1-2. The SCWR fuel assembly with metal water rod boxes, from [McDonald, 2005].

Table 1-4. Reference fuel pin design for the reference SCWR. From [McDonald, 2005].

Fuel pin outside diameter	10.2 mm
Fuel pin pitch	11.2 mm
Cladding thickness	0.63 mm
Cladding materials	TBD
Fuel pellet outside diameter	8.78 mm
Pellet to cladding gap (cold)	80 microns
Fuel composition	UO ₂ , 95% TD
Fuel density	10.4215 g/cc
Heated fuel length	4.27 m
Fission gas plenum length	0.6 m
Total fuel pin height	4.87 m
Fill gas pressure at room temperature	6.0 MPa

1.1 Neutronic computational model used in [McDonald, 2005]

The physics calculations in [McDonald, 2005] were performed using a 1/8th assembly model with the Monte Carlo code MCNP. A radial view of the MCNP model is shown in Figure 1-3. Depletion was performed with the 1-group, zero dimensional depletion code ORIGEN-2, coupled with MCNP.

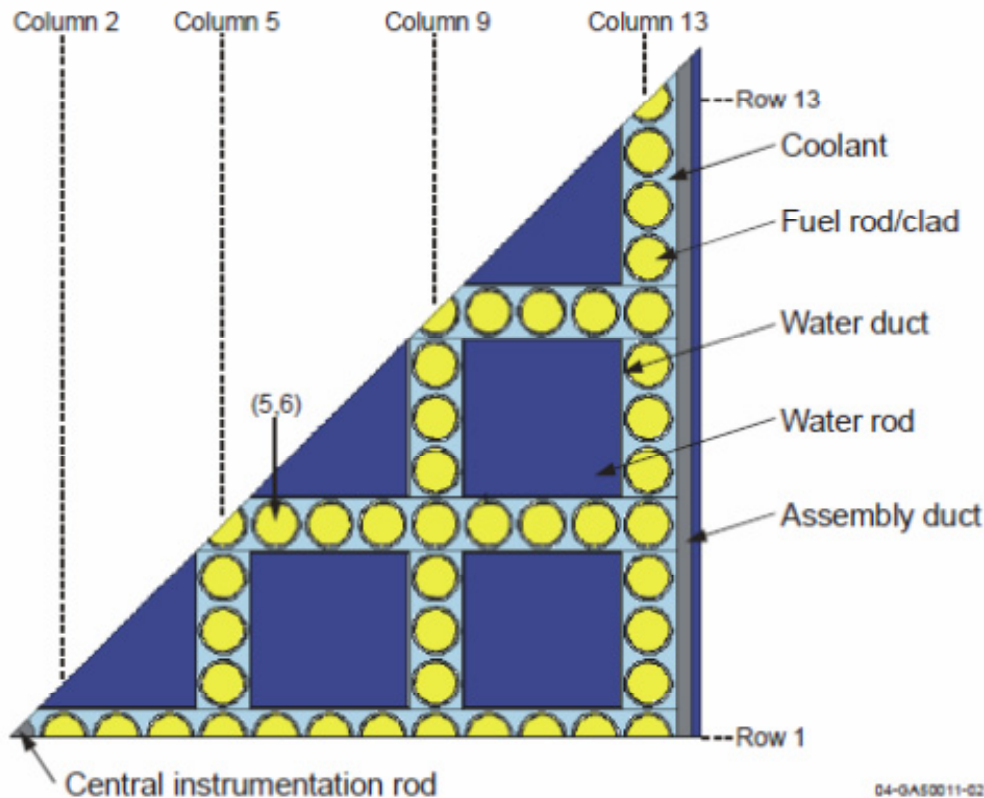


Figure 1-3. MCNP 1/8-assembly model of the 25×25 SCWR fuel assembly lattice showing the fuel rods, water rods, coolant channels.

The reference cladding material, also used for the channel boxes and for the assembly duct, is a special Oxide Dispersion Steel (ODS) known as MA956. The detailed composition of four cladding materials is shown in Table 1-5. The reason for the choice of this cladding material is not clear from [McDonald, 2005], since it appears to be a rather poor choice in terms of parasitic neutron capture (Table 1-6): it can be conjectured that the choice of MA956 could be related to superior mechanical and corrosion-resistant properties of MA956 as compared to Zr-4. A study was also reported in [McDonald, 2005] of a SCWR assembly design using SiC for ducts and cladding, which exhibits a substantially smaller parasitic absorption as compared to MA956. However, the SiC design was not considered “reference”: for this reason, the reference design for this study is MA956-based.

The fuel rods, water channels and assembly ducts are modeled explicitly in the MCNP model. The model is divided in 10 axial zones, each featuring a different water density for the coolant and the water channels, as shown in Table 1-7.

The top reflector is modeled as containing only water at the density shown in Table 1-7, as is the bottom mixing volume. The bottom 60 cm long fuel gas plenum is modeled explicitly: however, it was not found in [McDonald, 2005] a detailed description of the plenum model that could be replicated exactly in our Keno-V model. The standard plenums for LWR are filled with pressurized He, and there is a spring to hold the fuel in place. However, the SCWR plenum filling is expected to be different, because of its location below the fuel, which does not appear suitable for housing a spring. For these reasons, and because the exact details of the plenum model are not expected to have a material impact on the

neutronic properties calculated for the core, it was assumed in our model that the filling material is vacuum.

The 3 sides visible in Figure 1-3 have reflective boundary conditions, so as to model a radially infinite lattice of identical assemblies.

The water temperatures of the coolant and of the water channels are set at 527°C and the temperature of the fuel is set everywhere at 608°C, because of the availability of the cross sections at these temperatures in the MCNP libraries.

Table 1-5. Major elemental constituents for MA956, Alloy 718, Zircaloy-4, and SiC. From [McDonald, 2005].

Element	MA956 (Wt %)	Alloy 718 (Wt %)	Zr-4 (Wt %)	SiC (Wt %)
C		0.038	0.027	30.0
O	0.1488		0.120	
Al	5.75	0.49		
Si		0.19		70.0
Ti	0.60	0.91		
V		0.01		
Cr	21.5	19.08	0.10	
Mn		0.20		
Fe	71.45	18.122	0.21	
Ni		52.90	0.007	
Y	0.5512			
Zr			98.057	
Nb		5.05	0.012	
Mo		3.01		
Sn			1.45	
Density (g/cc)	7.25	8.19	6.57	2.9749

Table 1-6. Assembly lattice k-infinity for four different clad materials. From [McDonald, 2005].

Clad Material	K-infinity	Reactivity (ρ)
Zircaloy-4	1.425477 (0.0002)	--
MA956 (ODS)	1.266155 (0.0002)	-13.58
Alloy 718	1.153701 (0.0002)	-25.42
SiC	1.436039 (0.0002)	+0.79

Numbers in parentheses are the one-sigma statistical relative error.

Table 1-7 shows the converged water densities at BOL used in [McDonald, 2005]. It is noted that the coolant density decreases in going from the bottom to the top of the core from 0.54732 g/cm³ at the entrance of the active core region to 0.09171 g/cm³ at the exit of the upper plenum. The water density in the moderator water rods increases in going from the bottom of the core to the top, since it flows in the opposite direction as compared to the coolant. The axial profile of the fuel enrichment was chosen in [McDonald, 2005] to avoid a skewed axial power density, that would have been obtained if a uniform 5% enrichment was chosen instead (see Figure 1-4). This seem to suggest that the moderation could be

reduced in the top part of the core, thus reducing the size of the water rods and leaving more room available for active power generation, thus potentially improving the economic performance of this design.

Table 1-7. Converged beginning-of-life SCWR water densities for the coolant. From [McDonald, 2005].

Region	Lower Elevation (cm)	Upper Elevation (cm)	Coolant Density (g/cc)	Water Rod Density (g/cc)	UO ₂ Enrich (wt% ²³⁵ U)
Lower mixing or reflector	-90.48	-60.00	0.5649	0.5379	
Gas plenum	-60.00	0.00	0.5629	0.5363	
Fuel (bottom)	0.00	42.7	0.54732	0.5345	5.0
Fuel	42.7	85.4	0.49647	0.5375	5.0
Fuel	85.4	128.1	0.40936	0.5468	5.0
Fuel	128.1	170.8	0.30866	0.5608	5.0
Fuel	170.8	213.5	0.22573	0.5796	5.0
Fuel	213.5	256.2	0.17009	0.6044	5.0
Fuel	256.2	298.9	0.13481	0.6336	4.9
Fuel	298.9	341.6	0.11265	0.6683	4.8
Fuel	341.6	384.3	0.09918	0.7056	4.8
Fuel (top)	384.3	427.0	0.09200	0.7427	4.8
Upper reflector	427.0	457.48	0.09171	0.7779	

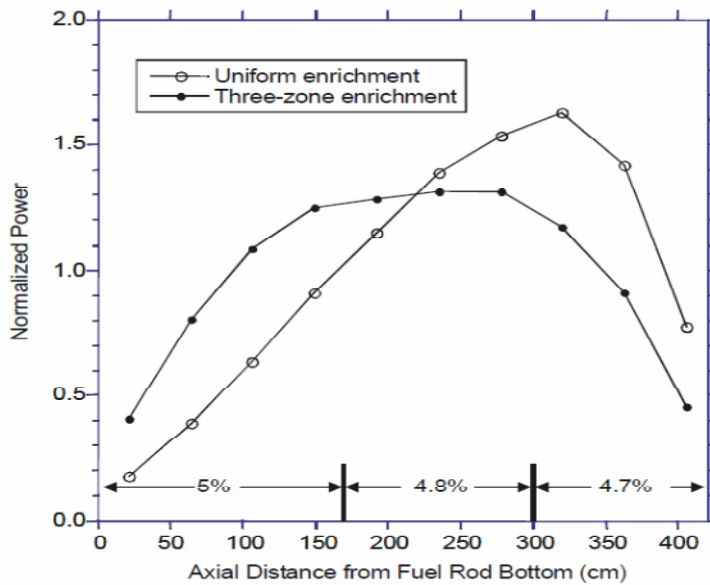


Figure 1-4. Axial power from [McDonald, 2005].

2. Description of the model

The full input of the TRITON/Keno-V is shown in Appendix A. To maximize the computational accuracy, a full assembly three-dimensional model has been modeled with the well benchmarked Monte Carlo code Keno-V. A radial view of the assembly model is shown in Figure 2-1: it is observed that all the fuel rods are modeled explicitly, including the fuel-cladding gap at nominal conditions. The assembly shroud and the interbundle gap are also explicitly modeled. The central instrumentation channels are occupied by water during the depletion analysis.

The active fuel region is divided in 10 zones of equal length (42.7 cm), consistently with the data in Table 1-7. The water densities of each coolant and moderator zones are shown in Figure 1-7, and are kept constant throughout the depletion analysis. For simplicity, the water channel ducts are not modeled explicitly, but the duct material is homogenized with the water in the channels. Since the self shielding effect of the duct materials is negligible, the homogenized model does provide an accurate representation of the system from a neutronic perspective. Since the wall channels take 4.71% of the volume of the water channels, the water density of Table 1-7 is reduced to 95.29% of the nominal value, while the remaining space is occupied by the isotopes of the ducts. Because of the large parasitic absorption of MA956 as compared to standard Zircaloy-4 (see Table 1-6 for the k_{inf} calculated at BOL using the MCNP model of [McDonald, 2005]), the composition of the cladding is accurately reproduced in the model used for this analysis.]

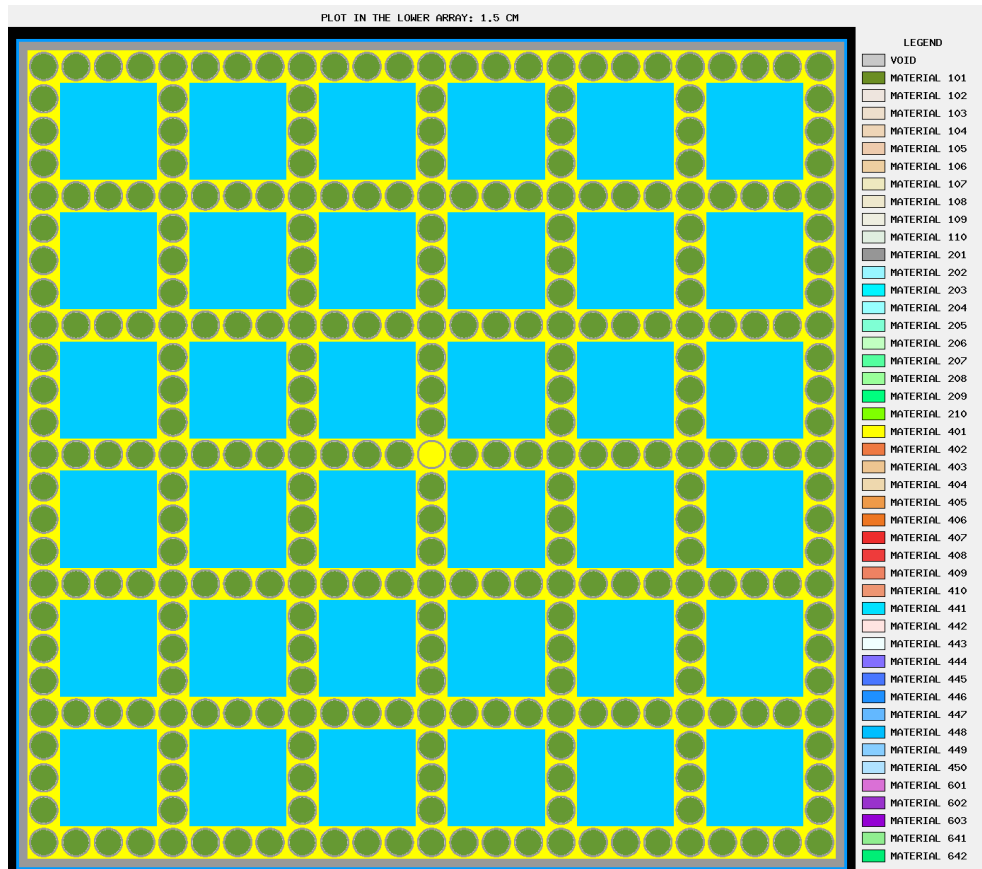


Figure 2-1. Radial view of the Keno-V full assembly model used for this work.

No information was found in [McDonald, 2005] on the water conditions in the inter-assembly gaps, which are 1 mm thick on each side of the assembly in Table 1-3. In fact, considerable uncertainties still are present in the final design and the numbers in Table 1-3 appear to be only tentative: “... a number of the dimensions are tentative, including the fuel bundle wall thickness, and the inter-assembly gap size and the fuel pin spacer have yet to be designed” [McDonald, 2005]. For simplicity, the water density in the inter-assembly gaps is assumed at the density of zone 6, or 0.5760 g/cm^3 , since it is close to the average of the axial density of the water channels. The neutronic effect of the water in the interassembly gap is expected to be minimal.

The UO_2 density is 10.4215 g/cm^3 as shown in Table 1-4. The fuel and water temperatures were set at 608°C and 527°C to match the parameters of the MCNP model of [McDonald, 2005] (see Section 1.1).

The bottom and top reflectors are modeled explicitly with the parameters indicated in Table 1-7. The density of the water in the water channels has been reduced to 95.29% of the nominal values shown in Figure 1-7, to allow the homogenization of the water channel ducts, as was done in the active fuel region. This allows an explicit modeling of the water channel ducts, even though the neutronic importance of structural materials in those regions is minimal. The boundary conditions above the upper reflectors and below the lower mixing or reflectors are void. The bottom 60 cm long fuel gas plenum is modeled explicitly with a tube representing the fuel-gas plenum, surrounded by water at the appropriate density.

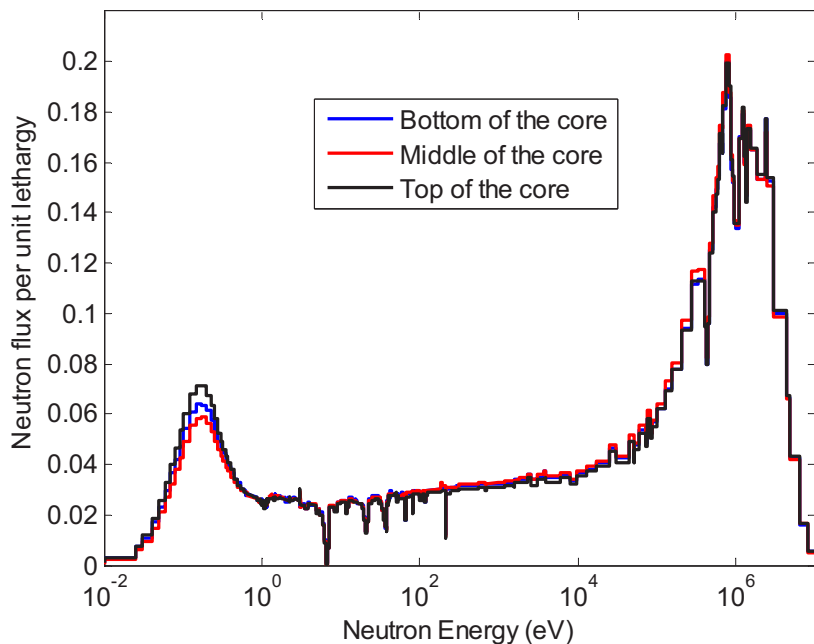


Figure 2-2. SCWR spectra at BOL in the fuel at the bottom, center and top of the core.

The depletion analysis was performed using both “Nitawl and ENDF/B-V” and “CENTRM and ENDF/B-VII” for the multigroup cross section generation. Because of the thermal spectrum of this core (see Figure 2-3), no substantial difference was observed between the results of the two cross section processing (see Figure 2-2 for a comparison of the k_{eff} evolution with burnup using the two cross section processing method). The ORIGEN-S depletion calculations are terminated at 49 GWD/MTiHM, since the single batch burnup (BU_1) is crossing 1 at 32.7 GWD/MTiHM. The actual burnup reached using a 3-batches shuffling scheme can be calculated approximately using the linear reactivity model: Equation 2.1

shows the burnup BU_n that would be obtained using an “*n*-batches” reshuffling scheme. Assuming that the SCWR would be operated on a 3-batches reshuffling, BU_3 would be equal to 49 GWD/MTiHM, or 3.894 EFPY at the nominal power density.

$$BU_n = BU_1 \cdot 2n / (n+1) \quad \text{Eq. 2-1}$$

The calculated axial power profile for the reference assembly is plotted in Figure 2-4, and is in good agreement with that indicated as “Three-zone enrichment” in Figure 1-4 from [McDonald, 2005].

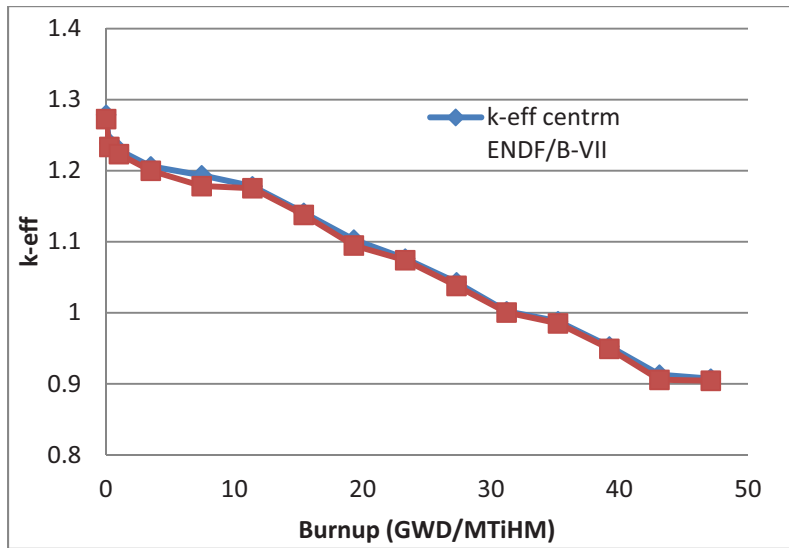


Figure 2-3. Evolution with burnup of the radially-averaged burnup, using both “Nitawl and ENDF/B-V” and “CENTRM and ENDF/B-VII” for the multigroup cross section generation.

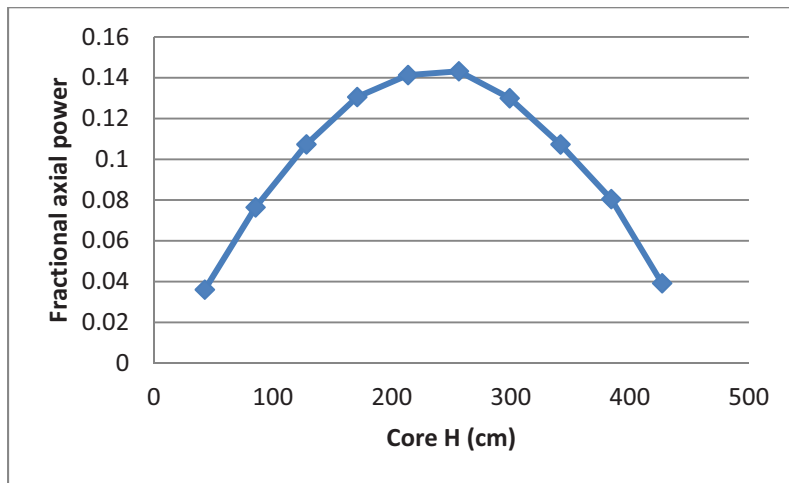


Figure 2-4. Axial power calculated by the Keno V model, to be compared to the axial power profile indicated as “Three-zone enrichment” in Figure 1-4 from [McDonald, 2005].

3. REFERENCES

- McDonald2005 Philip MacDonald, Jacopo Buongiorno, James W. Sterbentz, Cliff Davis, Robert Witt, Prof. Gary Was, J. McKinley, S. Teyseyre, Luca Oriani, Vefa Kucukboyaci, Lawrence Conway, N. Jonsson, Bin Liu, "Feasibility Study of Supercritical Light Water Cooled Reactors for Electric Power Production," INEEL/EXT-04-02530, January 2005.
- Piet2011 Steven J. Piet, Samuel E. Bays, David W. Gerts, Edward A. Hoffman, "Description of Transmutation Library for Fuel Cycle System Analyses (FY2011 update)," FCRD-SYSA-2010-000116, Rev1, INL/EXT-10-19545, Rev1, September 16, 2011.

APPENDIX A

TRITON/KENO-V input for the RBWR model

The TRITON/Keno-V model used for the reference depletion calculation is shown in this appendix. The Keno V execution with the number of neutrons specified in this input required a CPU time of approximately 10 minutes on a single Intel E8400@3GHz processor. The k-eff is calculated with a standard deviation of approximately 20 pcm. The attached input has been executed on SCALE5.1 and SCALE6.1, using both “nitawl and ENDF/B-V” and “centrm and ENDF/B-VII”. No substantial difference was observed in the calculated results using the two codes and cross section processing methods (see Figure 2-3). For this reason, the results using nitawl and ENDF/B-V were chosen for further processing, since they could be obtained using SCALE5.1. The author has used SCALE5.1 extensively in the past, and has better confidence in his understanding of the printed output, normalization factors etc... as compared to the just-released SCALE6.1

```
=t5-depl parm=(nitawl,addnux=3)
Title
238groupndf5
read comp
'
----- Fuels
' composition 101 (5.0 w/o U235)
o-16 101 0 0.0465138 881.15 end
u-235 101 0 0.0011769 881.15 end
u-238 101 0 0.0220800 881.15 end
'
' composition 102 (5.0 w/o U235)
o-16 102 0 0.0465138 881.15 end
u-235 102 0 0.0011769 881.15 end
u-238 102 0 0.0220800 881.15 end
'
' composition 103 (5.0 w/o U235)
o-16 103 0 0.0465138 881.15 end
u-235 103 0 0.0011769 881.15 end
u-238 103 0 0.0220800 881.15 end
'
' composition 104 (5.0 w/o U235)
o-16 104 0 0.0465138 881.15 end
u-235 104 0 0.0011769 881.15 end
u-238 104 0 0.0220800 881.15 end
'
' composition 105 (5.0 w/o U235)
o-16 105 0 0.0465138 881.15 end
u-235 105 0 0.0011769 881.15 end
u-238 105 0 0.0220800 881.15 end
'
' composition 106 (5.0 w/o U235)
o-16 106 0 0.0465138 881.15 end
u-235 106 0 0.0011769 881.15 end
u-238 106 0 0.0220800 881.15 end
'
' composition 107 (4.9 w/o U235)
o-16 107 0 0.0465132 881.15 end
u-235 107 0 0.0011534 881.15 end
u-238 107 0 0.0221032 881.15 end
'
' composition 108 (4.8 w/o U235)
o-16 108 0 0.0465126 881.15 end
u-235 108 0 0.0011299 881.15 end
u-238 108 0 0.0221264 881.15 end
'
' composition 109 (4.8 w/o U235)
o-16 109 0 0.0465126 881.15 end
u-235 109 0 0.0011299 881.15 end
u-238 109 0 0.0221264 881.15 end
'
' composition 110 (4.8 w/o U235)
o-16 110 0 0.0465126 881.15 end
u-235 110 0 0.0011299 881.15 end
u-238 110 0 0.0221264 881.15 end
'
'
' ----- cladding
'
O 201 DEN= 0.010788 1 800.15 end
Al 201 DEN= 0.416875 1 800.15 end
Ti 201 DEN= 0.043500 1 800.15 end
Cr 201 DEN= 1.538750 1 800.15 end
Fe 201 DEN= 5.180125 1 800.15 end
Y 201 DEN= 0.039962 1 800.15 end
'
O 202 DEN= 0.010788 1 800.15 end
Al 202 DEN= 0.416875 1 800.15 end
Ti 202 DEN= 0.043500 1 800.15 end
Cr 202 DEN= 1.538750 1 800.15 end
Fe 202 DEN= 5.180125 1 800.15 end
Y 202 DEN= 0.039962 1 800.15 end
```

```

,
O 203 DEN= 0.010788 1 800.15 end
Al 203 DEN= 0.416875 1 800.15 end
Ti 203 DEN= 0.043500 1 800.15 end
Cr 203 DEN= 1.558750 1 800.15 end
Fe 203 DEN= 5.180125 1 800.15 end
Y 203 DEN= 0.039962 1 800.15 end
,
O 204 DEN= 0.010788 1 800.15 end
Al 204 DEN= 0.416875 1 800.15 end
Ti 204 DEN= 0.043500 1 800.15 end
Cr 204 DEN= 1.558750 1 800.15 end
Fe 204 DEN= 5.180125 1 800.15 end
Y 204 DEN= 0.039962 1 800.15 end
,
O 205 DEN= 0.010788 1 800.15 end
Al 205 DEN= 0.416875 1 800.15 end
Ti 205 DEN= 0.043500 1 800.15 end
Cr 205 DEN= 1.558750 1 800.15 end
Fe 205 DEN= 5.180125 1 800.15 end
Y 205 DEN= 0.039962 1 800.15 end
,
O 206 DEN= 0.010788 1 800.15 end
Al 206 DEN= 0.416875 1 800.15 end
Ti 206 DEN= 0.043500 1 800.15 end
Cr 206 DEN= 1.558750 1 800.15 end
Fe 206 DEN= 5.180125 1 800.15 end
Y 206 DEN= 0.039962 1 800.15 end
,
O 207 DEN= 0.010788 1 800.15 end
Al 207 DEN= 0.416875 1 800.15 end
Ti 207 DEN= 0.043500 1 800.15 end
Cr 207 DEN= 1.558750 1 800.15 end
Fe 207 DEN= 5.180125 1 800.15 end
Y 207 DEN= 0.039962 1 800.15 end
,
O 208 DEN= 0.010788 1 800.15 end
Al 208 DEN= 0.416875 1 800.15 end
Ti 208 DEN= 0.043500 1 800.15 end
Cr 208 DEN= 1.558750 1 800.15 end
Fe 208 DEN= 5.180125 1 800.15 end
Y 208 DEN= 0.039962 1 800.15 end
,
O 209 DEN= 0.010788 1 800.15 end
Al 209 DEN= 0.416875 1 800.15 end
Ti 209 DEN= 0.043500 1 800.15 end
Cr 209 DEN= 1.558750 1 800.15 end
Fe 209 DEN= 5.180125 1 800.15 end
Y 209 DEN= 0.039962 1 800.15 end
,
O 210 DEN= 0.010788 1 800.15 end
Al 210 DEN= 0.416875 1 800.15 end
Ti 210 DEN= 0.043500 1 800.15 end
Cr 210 DEN= 1.558750 1 800.15 end
Fe 210 DEN= 5.180125 1 800.15 end
Y 210 DEN= 0.039962 1 800.15 end
,
,
,
water of the pin cells
H2O 601 DEN= 0.56490 1 800.15 end
H2O 602 DEN= 0.56290 1 800.15 end
,
H2O 401 DEN= 0.54732 1 800.15 end
H2O 402 DEN= 0.49647 1 800.15 end
H2O 403 DEN= 0.40936 1 800.15 end
H2O 404 DEN= 0.30866 1 800.15 end
H2O 405 DEN= 0.22573 1 800.15 end
H2O 406 DEN= 0.17009 1 800.15 end
H2O 407 DEN= 0.13481 1 800.15 end
H2O 408 DEN= 0.11265 1 800.15 end
H2O 409 DEN= 0.09918 1 800.15 end
H2O 410 DEN= 0.09200 1 800.15 end
,
H2O 603 DEN= 0.09171 1 800.15 end
,
,
,
water of the water rods (Density reduced to 95.29% of nominal no make space for channel ducts)
H2O 641 DEN= 0.51259 1 800.15 end
H2O 642 DEN= 0.51107 1 800.15 end
,
H2O 441 DEN= 0.50935 1 800.15 end
H2O 442 DEN= 0.51221 1 800.15 end
H2O 443 DEN= 0.52107 1 800.15 end
H2O 444 DEN= 0.53441 1 800.15 end
H2O 445 DEN= 0.55233 1 800.15 end
H2O 446 DEN= 0.57596 1 800.15 end
H2O 447 DEN= 0.60379 1 800.15 end
H2O 448 DEN= 0.63686 1 800.15 end
H2O 449 DEN= 0.67240 1 800.15 end
H2O 450 DEN= 0.70775 1 800.15 end
,
H2O 643 DEN= 0.74130 1 800.15 end
,
,
,
,
Cladding mixed into the water rods (density reduced to 4.71% of nominal)
,
O 641 DEN= 0.000508 1 800.15 end
Al 641 DEN= 0.019615 1 800.15 end

```

```

Ti 641 DEN= 0.002047 1 800.15 end
Cr 641 DEN= 0.073343 1 800.15 end
Fe 641 DEN= 0.243736 1 800.15 end
Y 641 DEN= 0.001880 1 800.15 end
,
O 642 DEN= 0.000508 1 800.15 end
Al 642 DEN= 0.019615 1 800.15 end
Ti 642 DEN= 0.002047 1 800.15 end
Cr 642 DEN= 0.073343 1 800.15 end
Fe 642 DEN= 0.243736 1 800.15 end
Y 642 DEN= 0.001880 1 800.15 end
,
,
O 441 DEN= 0.000508 1 800.15 end
Al 441 DEN= 0.019615 1 800.15 end
Ti 441 DEN= 0.002047 1 800.15 end
Cr 441 DEN= 0.073343 1 800.15 end
Fe 441 DEN= 0.243736 1 800.15 end
Y 441 DEN= 0.001880 1 800.15 end
,
O 442 DEN= 0.000508 1 800.15 end
Al 442 DEN= 0.019615 1 800.15 end
Ti 442 DEN= 0.002047 1 800.15 end
Cr 442 DEN= 0.073343 1 800.15 end
Fe 442 DEN= 0.243736 1 800.15 end
Y 442 DEN= 0.001880 1 800.15 end
,
O 443 DEN= 0.000508 1 800.15 end
Al 443 DEN= 0.019615 1 800.15 end
Ti 443 DEN= 0.002047 1 800.15 end
Cr 443 DEN= 0.073343 1 800.15 end
Fe 443 DEN= 0.243736 1 800.15 end
Y 443 DEN= 0.001880 1 800.15 end
,
O 444 DEN= 0.000508 1 800.15 end
Al 444 DEN= 0.019615 1 800.15 end
Ti 444 DEN= 0.002047 1 800.15 end
Cr 444 DEN= 0.073343 1 800.15 end
Fe 444 DEN= 0.243736 1 800.15 end
Y 444 DEN= 0.001880 1 800.15 end
,
O 445 DEN= 0.000508 1 800.15 end
Al 445 DEN= 0.019615 1 800.15 end
Ti 445 DEN= 0.002047 1 800.15 end
Cr 445 DEN= 0.073343 1 800.15 end
Fe 445 DEN= 0.243736 1 800.15 end
Y 445 DEN= 0.001880 1 800.15 end
,
O 446 DEN= 0.000508 1 800.15 end
Al 446 DEN= 0.019615 1 800.15 end
Ti 446 DEN= 0.002047 1 800.15 end
Cr 446 DEN= 0.073343 1 800.15 end
Fe 446 DEN= 0.243736 1 800.15 end
Y 446 DEN= 0.001880 1 800.15 end
,
O 447 DEN= 0.000508 1 800.15 end
Al 447 DEN= 0.019615 1 800.15 end
Ti 447 DEN= 0.002047 1 800.15 end
Cr 447 DEN= 0.073343 1 800.15 end
Fe 447 DEN= 0.243736 1 800.15 end
Y 447 DEN= 0.001880 1 800.15 end
,
O 448 DEN= 0.000508 1 800.15 end
Al 448 DEN= 0.019615 1 800.15 end
Ti 448 DEN= 0.002047 1 800.15 end
Cr 448 DEN= 0.073343 1 800.15 end
Fe 448 DEN= 0.243736 1 800.15 end
Y 448 DEN= 0.001880 1 800.15 end
,
O 449 DEN= 0.000508 1 800.15 end
Al 449 DEN= 0.019615 1 800.15 end
Ti 449 DEN= 0.002047 1 800.15 end
Cr 449 DEN= 0.073343 1 800.15 end
Fe 449 DEN= 0.243736 1 800.15 end
Y 449 DEN= 0.001880 1 800.15 end
,
O 450 DEN= 0.000508 1 800.15 end
Al 450 DEN= 0.019615 1 800.15 end
Ti 450 DEN= 0.002047 1 800.15 end
Cr 450 DEN= 0.073343 1 800.15 end
Fe 450 DEN= 0.243736 1 800.15 end
Y 450 DEN= 0.001880 1 800.15 end
,
,
O 643 DEN= 0.000508 1 800.15 end
Al 643 DEN= 0.019615 1 800.15 end
Ti 643 DEN= 0.002047 1 800.15 end
Cr 643 DEN= 0.073343 1 800.15 end
Fe 643 DEN= 0.243736 1 800.15 end
Y 643 DEN= 0.001880 1 800.15 end
,
,
end comp
,
,
,
,
,
read celldata
latticecell triangpitch fuelr=0.439 101 cladr=0.5100 201 pitch=1.120 401 end
latticecell triangpitch fuelr=0.439 102 cladr=0.5100 202 pitch=1.120 402 end
    
```

```

latticecell triangpitch fuelr=0.439 103 cladr=0.5100 203 pitch=1.120 403 end
latticecell triangpitch fuelr=0.439 104 cladr=0.5100 204 pitch=1.120 404 end
latticecell triangpitch fuelr=0.439 105 cladr=0.5100 205 pitch=1.120 405 end
latticecell triangpitch fuelr=0.439 106 cladr=0.5100 206 pitch=1.120 406 end
latticecell triangpitch fuelr=0.439 107 cladr=0.5100 207 pitch=1.120 407 end
latticecell triangpitch fuelr=0.439 108 cladr=0.5100 208 pitch=1.120 408 end
latticecell triangpitch fuelr=0.439 109 cladr=0.5100 209 pitch=1.120 409 end
latticecell triangpitch fuelr=0.439 110 cladr=0.5100 210 pitch=1.120 410 end
end celldata
,
read burndata
power=34.522 burn=14.484 down=0 nlib=1 end
power=34.522 burn=28.967 down=0 nlib=1 end
power=34.522 burn=114.90 down=0 nlib=1 end
end burndata
,
read depletion
101 102 103 104 105 106 107 108 109 110
end depletion
,
read rmoutput
bonami=yes nitawl=yes couple=yes
end rmoutput
,
read model
read parm
cfx=yes gen=3000 nsk=750 npg=3000 plt=yes flx=yes
end parm
,
read geom
,
----- Fuel segments channels
,
unit 101
cylinder 101 1 0.4390 42.7 0
cylinder 0 1 0.4470 42.7 0
cylinder 201 1 0.5100 42.7 0
cuboid 401 1 4p0.5600 42.7 0
,
unit 102
cylinder 102 1 0.4390 42.7 0
cylinder 0 1 0.4470 42.7 0
cylinder 202 1 0.5100 42.7 0
cuboid 402 1 4p0.5600 42.7 0
,
unit 103
cylinder 103 1 0.4390 42.7 0
cylinder 0 1 0.4470 42.7 0
cylinder 203 1 0.5100 42.7 0
cuboid 403 1 4p0.5600 42.7 0
,
unit 104
cylinder 104 1 0.4390 42.7 0
cylinder 0 1 0.4470 42.7 0
cylinder 204 1 0.5100 42.7 0
cuboid 404 1 4p0.5600 42.7 0
,
unit 105
cylinder 105 1 0.4390 42.7 0
cylinder 0 1 0.4470 42.7 0
cylinder 205 1 0.5100 42.7 0
cuboid 405 1 4p0.5600 42.7 0
,
unit 106
cylinder 106 1 0.4390 42.7 0
cylinder 0 1 0.4470 42.7 0
cylinder 206 1 0.5100 42.7 0
cuboid 406 1 4p0.5600 42.7 0
,
unit 107
cylinder 107 1 0.4390 42.7 0
cylinder 0 1 0.4470 42.7 0
cylinder 207 1 0.5100 42.7 0
cuboid 407 1 4p0.5600 42.7 0
,
unit 108
cylinder 108 1 0.4390 42.7 0
cylinder 0 1 0.4470 42.7 0
cylinder 208 1 0.5100 42.7 0
cuboid 408 1 4p0.5600 42.7 0
,
unit 109
cylinder 109 1 0.4390 42.7 0
cylinder 0 1 0.4470 42.7 0
cylinder 209 1 0.5100 42.7 0
cuboid 409 1 4p0.5600 42.7 0
,
unit 110
cylinder 110 1 0.4390 42.7 0
cylinder 0 1 0.4470 42.7 0
cylinder 210 1 0.5100 42.7 0
cuboid 410 1 4p0.5600 42.7 0
,
----- water channels
,
unit 441

```

```

cuboid 441 1 4p0.5600 42.7 0
|
unit 442
cuboid 442 1 4p0.5600 42.7 0
|
unit 443
cuboid 443 1 4p0.5600 42.7 0
|
unit 444
cuboid 444 1 4p0.5600 42.7 0
|
unit 445
cuboid 445 1 4p0.5600 42.7 0
|
unit 446
cuboid 446 1 4p0.5600 42.7 0
|
unit 447
cuboid 447 1 4p0.5600 42.7 0
|
unit 448
cuboid 448 1 4p0.5600 42.7 0
|
unit 449
cuboid 449 1 4p0.5600 42.7 0
|
unit 450
cuboid 450 1 4p0.5600 42.7 0
|
| ----- Instrumentation tubes
|
unit 541
cylinder 401 1 0.4390 42.7 0
cylinder 201 1 0.5100 42.7 0
cuboid 401 1 4p0.5600 42.7 0
|
unit 542
cylinder 402 1 0.4390 42.7 0
cylinder 202 1 0.5100 42.7 0
cuboid 402 1 4p0.5600 42.7 0
|
unit 543
cylinder 403 1 0.4390 42.7 0
cylinder 203 1 0.5100 42.7 0
cuboid 403 1 4p0.5600 42.7 0
|
unit 544
cylinder 404 1 0.4390 42.7 0
cylinder 204 1 0.5100 42.7 0
cuboid 404 1 4p0.5600 42.7 0
|
unit 545
cylinder 405 1 0.4390 42.7 0
cylinder 205 1 0.5100 42.7 0
cuboid 405 1 4p0.5600 42.7 0
|
unit 546
cylinder 406 1 0.4390 42.7 0
cylinder 206 1 0.5100 42.7 0
cuboid 406 1 4p0.5600 42.7 0
|
unit 547
cylinder 407 1 0.4390 42.7 0
cylinder 207 1 0.5100 42.7 0
cuboid 407 1 4p0.5600 42.7 0
|
unit 548
cylinder 408 1 0.4390 42.7 0
cylinder 208 1 0.5100 42.7 0
cuboid 408 1 4p0.5600 42.7 0
|
unit 549
cylinder 409 1 0.4390 42.7 0
cylinder 209 1 0.5100 42.7 0
cuboid 409 1 4p0.5600 42.7 0
|
unit 550
cylinder 410 1 0.4390 42.7 0
cylinder 210 1 0.5100 42.7 0
cuboid 410 1 4p0.5600 42.7 0
|
| ----- Reflector's fuel channels
|
unit 601
cuboid 601 1 4p0.5600 30.48 0
|
unit 602
cuboid 602 1 4p0.5600 60.00 0
|
unit 603
cuboid 603 1 4p0.5600 30.48 0
|
unit 641
cuboid 641 1 4p0.5600 30.48 0
|
unit 642
cuboid 642 1 4p0.5600 60.00 0
|
unit 643
cuboid 643 1 4p0.5600 30.48 0
|
|
global unit 16
array 1 -14.0 -14.0 0.0
cuboid 201 1 4p14.3 547.96 0
cuboid 446 1 4p14.4 547.96 0
|

```


APPENDIX B

OPUS input and nuclide concentrations post-processing

The OPUS input for the extraction of the nuclei associated with the TRITON/Keno-V input shown in Appendix A is shown in this appendix.

```
=opus  
title=Sum of all depletion materials  
units=gram  
  nrank=500  
libtype=all numunit=71 typarams=nuclides  
sort=no  
npos= 571 627 end  
end
```

The nuclei densities are stored in the ft71f001 file, in binary format.

OPUS can extract the nuclei concentrations at given “time dumps”. In this model there are 10 axial depletion zones; each depletion zone produces 57 time dumps based on the depletion story required in this case. The time dumps for all the zones combined are from 571 to 627. TRITON produces a summary table with a list of all time dumps: it can be obtained by searching “time dumps found on this set of libraries” and using the values in the 1st column, titled “Position”.

The file ft71f001 has to be in the temporary work directory of SCALE to be easily found. It is recommended, however, to save a copy of this file in the input/output directory for future reference.

If the volume of fuel is not entered, it is assumed to be (by default) that of 1 MT of HM of UO₂.

The downloaded inventory for all the zones combined, as calculated and extracted by OPUS, is correctly volume-weighted over the entire system. This was verified at BOL, when the weight enrichment for the fuel is known. The expected average enrichment of the assembly at BOL can be easily calculated to be 4.93%, matching exactly the value extracted by OPUS for the BOL masses at “time dump” 571.

A FORTRAN utility was created to collect the nuclei masses printed in the output and sort them in the same order as in the transmutation library maintained by the campaign.

APPENDIX C

XSECLIST input and cross sections post-processing

The one-group cross section can be extracted by the XSECLIST SCALE utility from the data saved in the binary files *ft33f001*. In the model used for this work there are 10 depletion zones, named 101 to 110, so 11 *ft33f001* files will be generated: *ft33f001.mix0101* to *ft33f001.mix0110*, plus one called *ft33f001.cmbined* which contains the flux-weighted cross sections for the entire system.

The manual of the XSECLIST utility is a section at the end of the ORIGEN-ARP manual, so it may be difficult to find if the location is not known “a priori” (Section D1.B.11).

The input of XSECLIST is the following:

```
=xseclist
SCWR_13.arplib
15
1
2
3
4
5
6
7
8
9
10
11
12
13
14
15
b
n
1022
10030
30060
30070
40090
40100
60140
270720
270730
270740
270750
280660
280720
280730
280740
280750
280760
280770
280780
290660
...
962440
962450
962460
962470
962480
962490
962500
962510
972490
972500
972510
982490
982500
982510
982520
982530
982540
982550
992530
992540
992541
992550
end
```

The name of the file “*SCWR_13.arplib*” is one of the *ft33f001* files (in this case *ft33f001.cmbined*) re-nominated with the “*arplib*” extension and located in the *C:/scale5.1/data/arplibs* directory for scale5.1, among the other pre-generated arplib data files.

15 is the number of burnup steps, and 1-15 list the burnup steps for which the cross sections are desired.

The list of nuclei contains the complete 1022 available nuclei list as sorted in the cross section libraries maintained by the campaign.

APPENDIX D

SCALE_XSLIST_READER for the conversion of OPUS and XSECLIST outputs to the standard format of the transmutation library

A FORTRAN utility was created to collect the cross sections printed in the output and sort them in the same order as in the cross section library maintained by the campaign. The most recent version of the utility (SCALE_XSLIST_READER.exe) was created on 21st June 2012.

The input of the utility is in a file called *list.inp*, the (partial) input of which is listed below:

```
!Isotope List
type="xsec"
"n 1022
inp="xseclist_15.out"
version="scale5"
START
H3
H36
L17
Li7
Be9
Be10
C14
Co72
Co73
Co74
Co75
Ni66
Ni72
Ni73
Ni74
Ni75
Ni76
...
...
CM248
CM249
CM250
CM251
BK249
BK250
BK251
CF249
CF250
CF251
CF252
CF253
CF254
CF255
ES254
ES254M
ES255
SF250
END
```

- The **type** keyword can assume the values *xsec* or *opus* for, respectively, sorting the 1 group cross sections or the nuclei densities;
- The **1022** value is number of nuclei for which data are extracted, and are listed after the **START** keyword in the correct order of desired sorting;
- The **input** keyword contains the opus of xseclist output file, input to this converter;
- The **version** keyword can assume the values *scale5* or *scale6* for, respectively, SCALE5.1 output and SCALE 6.0 or SCALE6.1 outputs.

The output of the sorting will be called *opus-converted.out* or *xsec-converted.out*.

The nuclei sums in the *opus-converted.out* output are not calculated, but copied from the opus output. The actual total mass of the nuclei can be different from the value reported in the *opus-converted.out*, for example, because the ¹⁶O mass in UO₂ fuel is not included in the transmutation library. The masses are not normalized, so they will need to be divided by the total mass calculated externally to the subroutine. This is an example where SCALE5.0, SCALE5.1 and SCALE6.0 differ from SCALE6.1: in SCALE6.1

the extracted cross sections are already calculated over the entire spectrum, so they do not need to be re-normalized.

Regarding the XS post processing (rows: nuclei, columns: burnup steps), the values are not in barns. They will need to be multiplied by the ratio of thermal to total fluxes to obtain barns. The thermal and total fluxes can be obtained by the Transport tables in the standard TRITON output: the one at Burnup=0 GWD/MTiHM is reported, as an example, below.

```

--- Material powers for depletion pass no. 0 (MW/MTHM) ---
Time = 0.00 days ( 0.000 y), Burnup = 0.00 Gwd/MTU, Transport k=1.27841

```

Mix No.	Total Power	Fractional Power	Mixture Power	Mixture Thermal Flux	Mixture Total Flux
101	1.014	0.02938	10.142	8.2707E+12	6.5535E+13
102	2.163	0.06264	21.626	1.7533E+13	1.4416E+14
103	3.233	0.09366	32.332	2.6161E+13	2.2050E+14
104	4.230	0.12254	42.304	3.4144E+13	2.9412E+14
105	4.777	0.13837	47.769	3.8582E+13	3.3549E+14
106	5.107	0.14794	51.073	4.1463E+13	3.5758E+14
107	4.914	0.14235	49.141	4.0894E+13	3.4013E+14
108	4.130	0.11963	41.298	3.5351E+13	2.8017E+14
109	3.031	0.08781	30.314	2.6141E+13	1.9990E+14
110	1.511	0.04378	15.113	1.3168E+13	9.5197E+13
201	0.107	0.00309	0.000	1.7364E+13	1.6279E+14
202	0.013	0.00039	0.000	1.9055E+13	1.4396E+14
203	0.020	0.00059	0.000	2.8396E+13	2.2021E+14
204	0.026	0.00076	0.000	3.6972E+13	2.9371E+14
205	0.029	0.00085	0.000	4.1735E+13	3.3499E+14
206	0.031	0.00091	0.000	4.4748E+13	3.5701E+14
207	0.031	0.00090	0.000	4.4111E+13	3.3938E+14
208	0.027	0.00077	0.000	3.8018E+13	2.7974E+14
209	0.020	0.00057	0.000	2.8105E+13	1.9938E+14
210	0.010	0.00028	0.000	1.4177E+13	9.4959E+13
401	0.001	0.00002	0.000	9.4858E+12	6.5412E+13
402	0.001	0.00004	0.000	2.0156E+13	1.4410E+14
403	0.002	0.00005	0.000	2.9955E+13	2.2053E+14
404	0.002	0.00005	0.000	3.8825E+13	2.9379E+14
405	0.001	0.00004	0.000	4.3703E+13	3.3513E+14
406	0.001	0.00003	0.000	4.6746E+13	3.5734E+14
407	0.001	0.00002	0.000	4.5944E+13	3.3967E+14
408	0.001	0.00002	0.000	3.9563E+13	2.7989E+14
409	0.000	0.00001	0.000	2.9168E+13	1.9957E+14
410	0.000	0.00000	0.000	1.4691E+13	9.4946E+13
441	0.002	0.00006	0.000	1.2361E+13	6.7100E+13
442	0.004	0.00013	0.000	2.6378E+13	1.4758E+14
443	0.007	0.00019	0.000	3.9632E+13	2.2592E+14
444	0.009	0.00025	0.000	5.2148E+13	3.0132E+14
445	0.010	0.00029	0.000	5.9637E+13	3.4394E+14
446	0.020	0.00057	0.000	5.2484E+13	3.1599E+14
447	0.011	0.00033	0.000	6.4168E+13	3.4958E+14
448	0.010	0.00029	0.000	5.5869E+13	2.8866E+14
449	0.008	0.00022	0.000	4.1738E+13	2.0650E+14
450	0.004	0.00011	0.000	2.1155E+13	9.8568E+13
601	0.000	0.00000	0.000	2.3033E+10	3.1319E+10
602	0.000	0.00001	0.000	4.2420E+12	6.3922E+12
603	0.000	0.00000	0.000	1.0386E+13	1.7805E+13
641	0.000	0.00000	0.000	2.3592E+10	3.3015E+10
642	0.001	0.00003	0.000	4.4039E+12	6.5782E+12
643	0.001	0.00004	0.000	1.1102E+13	1.7943E+13
Total	34.522	1.00000			

In the case of this study, where there are multiple mixtures, it was decided (somewhat arbitrarily) to use the ratio of the sums of the thermal and total fluxes of all the zones as a normalization factor.